***Oncogene* ONC-2020-01144 Revised Version R1**

Extramammary Paget's disease patient-derived xenografts harboring ERBB2 S310F mutation show sensitivity to HER2-targeted therapies

Takuya Maeda[1¶], Shinya Kitamura[1¶], Hiroshi Nishihara[2], Teruki Yanagi[1*]

[1] *Department of Dermatology, Faculty of Medicine and Graduate School of Medicine, Hokkaido University, Sapporo, Japan*

[2] *Genomics Unit, Keio Cancer Center, Keio University School of Medicine, Tokyo, Japan*

*Correspondence to Teruki Yanagi, M.D., Ph.D.

Department of Dermatology, Faculty of Medicine and Graduate School of Medicine, Hokkaido University, N15 W7, Kita-ku, Sapporo 060-8638, Japan

Telephone: +81-11-706-7387

Facsimile: +81-11-706-7820

E-mail: yanagi@med.hokudai.ac.jp

[¶] These authors contributed equally to this work.

Word count: 200-word abstract, 2899-word text

References: 39

Tables: 0

Figures: 5

Supplementary figures: 7

Supplementary tables: 2

Running title: A novel experiment model for extramammary Paget’s disease

Abbreviations:

EMPD: extramammary Paget’s disease

G: generation

HE: hematoxylin and eosin

LOH: loss of heterozygosity

PDX: patient-derived xenograft

TUNEL: terminal deoxynucleotidyl transferase dUTP nick end labeling

VAF: variant allele frequency

Abstract

Although the prognosis of advanced extramammary Paget's disease (EMPD) is poor, there have been no preclinical research models for the development of novel therapeutics. This study aims to establish a preclinical research model for EMPD. We transplanted EMPD tissue into immunodeficient NOD/Scid mice. Histopathological and genetic analyses using a comprehensive cancer panel were performed. For *in vivo* preclinical treatments, trastuzumab, lapatinib, docetaxel, or eribulin were administered to patient-derived xenograft (PDX) models. Tissue transplanted from the EMPD patient was enlarged in NOD/Scid mice and was transplanted into further generations. Both the transplantation of PDX into *nu/nu* mice and the reanimation of the cryopreserved xenografted tumors in NOD/Scid mice were successful. We also established an EMPD-PDX-derived primary cell culture. Histopathologically, the xenografted tumors were positive for CK7, which was consistent with the patient's tumors. Genetically, the pathogenic mutation *ERBB2* S310F was detected in the patient's tumors (primary intraepidermal lesion, metastatic lymph node) and was observed in the xenografted tumors even after continued passages. The xenografted tumors responded well to trastuzumab and lapatinib therapy. Also, cytotoxic agents (docetaxel and eribulin) were effective against the xenografted tumors. This PDX model (EMPD-PDX-H1) could be a powerful tool for the research and development of EMPD treatments.

Introduction

Paget's disease is a rare adnexal neoplasm that was first described by Sir James Paget in 1874 (ref. 1). Extramammary Paget's disease (EMPD) is a variant that is commonly seen in the genital areas and anus among the senior population (ref. 2), and the number of cases has been increasing in recent years (ref. 3). In most EMPD cases, tumor cells are localized in the epidermis, and the prognosis is relatively favourable (ref. 4). However, once tumor cells invade the dermis, patients are at a risk of lymph node and visceral metastases, and the prognosis becomes significantly poorer (ref. 5-7). A multi-center retrospective study by Ohara et al. showed that the 5-year survival rate for EMPD patients with distant metastasis was only 7% (ref. 7). There have been several retrospective studies on treatments for metastatic EMPD, such as cytotoxic chemotherapies (ref. 8-12), and small molecular inhibitors (ref. 13-15). However, the efficacies of these treatments have been evaluated only in single case reports or case series containing small numbers of patients. Thus, the development of novel therapeutic strategy for advanced EMPD has been desired.

In recent years, the usefulness of patient-derived xenograft (PDX) models has been reported in many types of cancers (ref. 16-18). PDX models have demonstrated an ability to maintain the characteristics of the original tumor and to be useful for preclinical therapeutic studies in certain cancers. These models have shown to be

predictive of clinical outcomes and are being used for preclinical drug evaluation, biomarker identification, biological studies, and personalized medicine strategies (ref. 17). For EMPD, Nishi et al. reported the first PDX model using an EMPD tumor in 1992 (ref. 19). They transplanted metastatic EMPD tissue into nude mice (*nu/nu* mice). Reportedly, their xenografted tumor maintained the histopathological features of the patient's original tumor, and they investigated the effect of hormonal stimulation on tumor growth. To the best of our knowledge, no additional studies using this PDX model have been published. Thus, no preclinical research models of EMPD including cell lines and PDX are currently available.

Here, we report a novel PDX model of EMPD (EMPD-PDX-H1) harboring a pathogenic *ERBB2* mutation. We performed histopathological and genetic analyses to confirm that the xenografted tumors maintained the characteristics of the patient's original tumors. Further, we performed treatment experiments using cytotoxic agents and HER2-targeted therapies.

Results

Establishment of the EMPD-PDX-H1

A schematic of the present study is shown in Figure 1. To establish a patient-derived EMPD xenograft, surgically resected tissue was transplanted onto the flanks of NOD/Scid mice (Figure 2 A, B). The transplanted EMPD tumor tissue grew into a firm nodule of more than 10 mm in diameter over the course of 5 months (generation 0: G0, Figure 2C). The xenograft tissue was analyzed by HE staining and immunohistochemistry for CK7 and HER2, and for androgen, estrogen and progesterone receptors. The EMPD-PDX-H1 tissue exhibited similar morphology and protein expressions to those of the patient's tissues (primary tumor and metastatic lymph node) (Figure 2D and Supplementary Figure S1). Once the tumor volume reached 500–1000 mm^3, the EMPD-PDX-H1 tumors were transplanted into the next generation of NOD/Scid mice. By the third passage, the growth volume curve of PDX in each generation became stable (Supplementary Figure S2). Also, we transplanted EMPD-PDX-H1 tumors into *nu/nu* mice. Both the transplantation of EMPD-PDX-H1 tumors into the *nu/nu* mice (3/3, 100%) and the reanimation of the cryopreserved EMPD-PDX-H1 tumors in the NOD/Scid mice (10/12, 83.3 %) were successful (Supplementary Figure S3 and S4). Also, we established primary culture cells from the 3^{rd} generation of EMPD-PDX-H1, in which cultured tumor cells were round or cuboidal

(Supplementary Figure S5).

EMPD-PDX-H1 harbors an *ERBB2* S310F mutation identical to that of the patient's tumors

To investigate the characteristics of EMPD-PDX-H1 and the similarity between the patient's tissues (primary tumor and metastatic lymph node) and EMPD-PDX-H1, we performed gene mutation analysis. To compare the cancer-associated genomic profile of the patient's tumors to those of their corresponding xenografts, we performed deep sequencing using a comprehensive cancer panel. EMPD-PDX-H1 tumors faithfully maintained the pathogenic genomic DNA alterations of *ERBB2* (c.929C>T, p.S310F), which was observed in the corresponding tumor (metastatic lymph node) of the patient (Figure 3A). *ERBB2* S310F mutation was conserved even after continued passages of EMPD-PDX-H1 (Figure 3A, PDX (G2)). Sanger sequencing targeting *ERBB2* mutation revealed that the patient's primary tumor (resected 12 years earlier) harbored the identical *ERBB2* S310F mutation (Figure 3B).

In addition to *ERBB2* S310F being retained in EMPD-PDX-H1, so were *TP53* A161T and *RB1* S780*. In the patient's lymph nodes, the variant allele frequency (VAF) for *TP53* A161T was 50.4% and for *RB1* S780* was 42.5%. The VAF of both mutations in EMPD-PDX-H1 was elevated to 100% (Supplementary Table S1). This is because

the normal allele was lost and the proportion of normal cells decreased in EMPD-PDX-H1 tumor. The mutation of *NF1* D2545N was also retained in EMPD-PDX-H1; however, its VAFs (47.5% in G1 and 50.3% in G2) suggest that the normal allele was sustained. *NOTCH1* S1409N has been observed in EMPD-PDX-H1 tumors (G1 and G2) with high VAF, possibly due to the loss of heterozygosity (LOH). Since no such mutation was detected in the patient's tumor, it might be crucial for PDX implantation.

Treatment experiments using EMPD-PDX-H1

Preclinical studies for EMPD have not been reported until this paper, possibly due to the unavailability of EMPD cell lines/PDX tissues. We performed treatment experiments to investigate whether EMPD-PDX-H1 responds to targeted therapies and chemotherapies as reported in clinical settings (Ref. 8-15). For the targeted therapy, since the PDX harbored pathogenic *ERBB2* S310F, we treated the tumor with HER2-targeted therapies (trastuzumab, lapatinib, and combination of the two). The single use of trastuzumab or lapatinib was found to suppress tumor progression, but the combined therapy was found to remarkably inhibit tumor growth (Figure 4, A–F). Regarding cytotoxic chemotherapies, the xenografted model responded well to docetaxel (Figure 5, A, B), which is reported to be effective against metastatic EMPD (Ref. 10, 11). We tested eribulin monotherapy, which has been shown to be effective as a second-line treatment

for breast cancer (ref. 20). Eribulin therapies (1.5 mg/kg/week) eliminated EMPD-PDX-H1 completely, and no relapse was observed for one week (Figure 5 C, D). We administered 0.45 mg/kg/week eribulin and obtained similar results (Figure 5 E, F). The results of treatment experiments were also confirmed by Ki-67 staining and terminal deoxynucleotidyl transferase dUTP nick end labeling (TUNEL) assays. In Ki-67 staining, all of the treated EMPD-PDX-H1 tumors showed a significantly lower ratio of positive cells than the non-treated tumors showed (Supplementary Figure S6). In the TUNEL assays, all of the treated EMPD-PDX-H1 tumors showed a significantly higher ratio of TUNEL-positive tumor cells than the control tumor cells showed (Supplementary Figure S7).

Discussion

The present study presented an EMPD PDX model that reproduced the patient's original tumor morphologically and genetically. We also reported the promising potency of HER-2 targeted therapies and cytotoxic chemotherapies.

It has been reported that certain EMPD cases revealed overexpression of HER2 as assessed by immunohistochemistry and *in situ* hybridization (ref. 21-23). In addition, somatic mutations analyses of EMPD have detected *ERBB2* mutations (ref. 24, 25). Overexpression of HER2 protein and *ERBB2* gene amplification positively correlate with disease progression (ref. 22). Clinically, several case reports have shown the efficacy of HER2-targeted therapies such as lapatinib and trastuzumab against metastatic EMPD (ref.13-15). In light of these facts, the HER2 signalling pathway is considered to contribute to carcinogenesis in HER2-positive/mutated EMPD. In the present study, the PDX model was found to harbor a pathogenic *ERBB2* mutation (S310F) without definitive amplification. *ERBB2* S310F mutation corresponds to the extracellular domain of ERBB2/HER2, and that domain has been reported as having the most common mutation of *ERBB2* in various cancers such as breast, lung, bladder, and colon (ref. 26). Greulich et al. reported that *ERBB2* S310F mutation leads to ERBB2/HER2 activation via two distinct mechanisms, characterized by elevated C-terminal tail phosphorylation or by covalent dimerization through intermolecular

disulfide bond formation (ref. 27). The S310F mutation has been reported in *ERBB2* non-amplified breast cancer and is not necessarily accompanied by *ERBB2* amplification (ref. 28). Also, HER2-targeted therapy is effective against lung, colon, and other cancers harboring the S310F mutation (ref. 27, 29, 30). Concerning EMPD, Mishra et al. were the first to report a case of EMPD harboring the *ERBB2* S310F mutation in which trastuzumab and capecitabine combination therapy was remarkably effective against multiple metastatic lesions (ref. 15). This case report is consistent with our experimental results showing that EMPD-PDX-H1 harboring *ERBB2* S310F is sensitive to HER2-targeted therapies. In addition, a phase 2 clinical study using trastuzumab combined with docetaxel for HER2-positive EMPD (UMIN000021311) is under way at Keio University in Japan.

The present study has also demonstrated the antitumor effects of cytotoxic chemotherapies. We herein tried the administration of eribulin, an inhibitor of microtubule dynamics that has proven effective against breast cancer (ref. 20, 31), since recent studies suggest that EMPD and mammary Paget's disease (a breast cancer) harbor common recurrent mutations (ref 24, 32). The eribulin administration showed high efficacy against all of EMPD-PDX-H1 tumors. Although there are no clinical reports of eribulin being effective against EMPD-PDX-H1, it is suggested that eribulin may be a treatment option for EMPD.

Unfortunately, we established the EMPD-PDX from only one patient in the present study due to the small number of advanced EMPD cases. In the future, it is necessary to confirm whether PDX models can be established from other patients using the same methods and to conduct treatment experiments on other PDX models to develop preclinical studies. Despite this limitation, EMPD-PDX-H1 is the first to investigate the efficacy of antitumor agents and to help in the search for new treatments for advanced EMPD.

In summary, we generated a novel EMPD PDX model that maintained the original patient's tumors both histopathologically and genetically. Our therapeutic experiments revealed *in vivo* tumor growth inhibition by anti-HER2 therapies (lapatinib and trastuzumab) and cytotoxic agents (docetaxel and eribulin). EMPD-PDX-H1 could be useful for developing effective therapies for EMPD.

Materials and Methods

Samples from the EMPD patient

EMPD tissues were obtained from inguinal lymph node metastases of a 78-year-old Japanese female whose primary genital skin lesion had been removed 12 years before the lymph node metastasis occurred (Figure 2 A, B). She had no significant familial or past medical history. The resected metastatic lymph node was separated into two parts: One was immediately transported on ice for transplantation, and the other was fixed in formalin and embedded into paraffin for pathological diagnosis. Written informed consent was obtained from the patient, and this research was approved by the Ethics Committee of Hokkaido University Hospital in accordance with the Declaration of Helsinki (IRB approval number: 018-0424).

Establishment of EMPD-PDX-H1

A 10-mm-wide piece of EMPD tissue was subcutaneously transplanted with Matrigel (BD Bioscience, Franklin Lakes, NJ, USA) onto both flanks of a 5-week-old female NOD/Scid mouse (Clea, Tokyo, Japan). The mice in this study were housed in a specific pathogen-free condition at a fixed temperature (22–25°C) and were held on a 12-hour light-dark cycle. The mice were given distilled water and standard chow *ad libitum*. Animal use procedures were approved by the institutional committee of Hokkaido

University (approval numbers 19-0015 and 19-0093). The tumor-transplanted mouse was observed twice a week for 5 months. The tumors were measured once a week by caliper. Tumor volume was calculated using the following formula: (long axis x short axis^2)/2 (ref. 33). Once the tumor volume reached 500–1000 mm^3, EMPD-PDX-H1 tumors were transplanted into the next generation of NOD/Scid mice. In the first two consecutive mouse-to-mouse passages, EMPD-PDX-H1 tumors were separated into three sections: The first part was cut into pieces (less than 5 mm in diameter) for transplantation, and the second part was frozen immediately at −80 °C for DNA extraction and was fixed in formalin and then embedded into paraffin for pathological analysis. Treatment experiments were performed on the 3rd–5th generations. At the 4th passage, transplantation was also performed on 5-week-old female nude (*nu/nu*) mice (Clea, Tokyo, Japan). Greater amounts of fresh tumor pieces at passages 4 and 5 were frozen in CryoStor® CS10 (BioLife Solutions, Owego, NY, USA) and stored at −80 °C (ref. 34). The cryopreserved EMPD-PDX-H1 tumors were re-transplanted into NOD/Scid mice to confirm reanimation.

Histopathological analyses

Formalin-fixed, paraffin-embedded tissue sections of the patient's tumors or the xenografted tumors were cut into 4-μm sections. Hematoxylin and eosin (HE) staining

as well as immunohistochemistry for CK7 (Dako, Code. M7018, Denmark), HER2 (Dako, Code. A0485, Denmark), androgen receptor (ScyTek laboratories, RA0012-C, USA), estrogen receptor (Leica Biosystems, NCL-L-6F11, UK), progesterone receptor (Leica Biosystems, NCL-L-PGR-312, UK) and Ki-67 (Abcam, #ab8191) were performed to compare the histopathology of the primary lesions, metastatic lymph nodes, and xenografts. DAB chromogen was applied to yield a brown color (ref. 35). For nuclear Ki-67 expression, the percentage of positive cells among at least 100 cancer cells from three randomly selected fields of vision using a high-power lens (x 400) were calculated. The expression levels of HER2 protein were evaluated according to the HER2 testing guideline for breast cancer as follows (ref. 36).

3+: “circumferential membrane staining that is complete, intense”

2+: “circumferential membrane staining that is incomplete and/or weak to moderate and within > 10% of the invasive tumor cells or complete and circumferential membrane staining that is intense and within ≤ 10% of the invasive tumor cells”

1+: “incomplete membrane staining that is faint or barely perceptible and within > 10% of the invasive tumor cells”

0: “no staining observed or membrane staining that is incomplete and is faint or barely perceptible and within ≤ 10% of the invasive tumor cells”

TUNEL assays

Cell death was assessed by the TUNEL method using an In Situ Cell Death Detection Kit (Roche, #11684817910) according to the manufacturer's instructions. For nuclear TUNEL staining, the percentage of positive cells among at least 100 cancer cells from three randomly selected fields of vision using a high-power lens (x 400) was calculated.

Gene mutation analysis

EMPD patient tissues and EMPD-PDX-H1 tissues were pathologically reviewed to ensure that the tumor cell content was high enough and that no significant tumor necrosis had occurred before DNA extraction. Genomic DNA was extracted from our patient's blood and from each tissue sample using the DNA Mini Kit (QIAGEN, Cat#51304, Germany) or the GeneRead FFPE DNA Kit (QIAGEN, Cat#180134, Germany). The quantity and purity of DNA samples were measured using a Nanodrop ND-1000 UV/VIS Spectrophotometer (Thermo Scientific, USA). DNA fragment integrity was confirmed by electrophoresis using 1% agarose gel. The concentrations of DNA samples were normalized to 20 ng/μl, and those samples were stored at −20°C until use. Genomic testing was performed at the genomic unit of the Keio Cancer Center in Tokyo, Japan. After the quality of the DNA was checked based on the DNA integrity number (DIN) score calculated using the Agilent 2000 TapeStation (Agilent

Technologies, Waldbronn, Germany), targeted amplicon exome sequencing for 160 cancer-related genes was performed using the Illumina MiSeq sequencing platform (Illumina, San Diego, CA). The list of 160 cancer-related genes included in the comprehensive cancer panel is shown in Supplementary Table S2. The minimum amount of DNA was 50 ng, and the minimum quality for DNA was that with a DIN score over 3.1. The sequencing data were analyzed using an original bioinformatics pipeline called GenomeJack (Mitsubishi Space Software, Tokyo, Japan). In addition, we performed mutation analysis by Sanger sequencing to confirm the pathogenic *ERBB2* gene alteration in the primary lesions using the following primers: forward primer 5'-CGGTAATGCTGCTCATGGTG-3' and reverse primer 5'-CTTGCTGCACTTCTCACACC-3'.

EMPD-PDX-H1-derived primary cell culture

Tumor tissue from EMPD-PDX-H1 mice (3^{rd} generation) was minced and washed with PBS repeatedly. The minced tissue was directly plated onto dishes coated with type I collagen (Iwaki, Tokyo, Japan) in a medium of RPMI (Nakalai, Kyoto, Japan) containing 10% fetal bovine serum (FBS, Sigma).

Treatment experiments using EMPD-PDX-H1

Tumor growth curves for all EMPD-PDX-H1 were generated using the kinetic measurement of tumor volumes. The tumor volume range of 50 to 100 mm^3 in the tumor-bearing NOD/Scid mice was randomized, and treatment experiments were begun. All treatment experiments were performed with a minimum of n = 4 mice per condition. Control mice were administered with 100 μl of 0.5% hydroxypropyl methylcellulose once a day orally (n = 5), intraperitoneally injected with 100 μl of PBS twice per week (n = 5), or intravenously injected with 100 μl of PBS once per week (n = 5). In the HER2-targeted treatments, trastuzumab (10 mg/kg, Herceptin®, Chugai Pharmaceutical Co., Ltd., Tokyo, Japan) was given intraperitoneally twice weekly according to a previous study (ref. 37). Lapatinib (100 mg/kg, CS-0036, Chem Scene, USA) was administered once a day orally in 0.5% hydroxypropyl methylcellulose and 0.1% Tween 80 (P1754, Sigma-Aldrich, Germany) (ref. 38). We also administered trastuzumab and lapatinib in combination (ref. 37). Concerning cytotoxic agents, docetaxel (20 mg/kg, Santa Cruz Biotechnology, CA, USA, #sc-201436) and eribulin (1.5 or 0.45 mg/kg, Halaven, Eisai Co., Ltd., Tokyo, Japan) were administered intravenously once per week (ref. 31, 39). Tumor volumes were measured once a week by caliper, and tumor weights were measured with a scale at 28 days after treatment initiation. Tumor volume and weight were recorded in a blinded manner.

Statistical analysis

To evaluate the statistical significance of the treatment experiments, Student's *t*-test was used to compare tumor volume between the treatment groups and the control group. Statistical tests were two sided, with $P < 0.05$ considered significant.

Disclosure of Potential Conflicts of Interest

None to declare.

Acknowledgments

We thank Ms. Yuko Tateda for her technical assistance. This work was supported in part by KAKENHI grant #18K08259 to T. Yanagi from the Ministry of Education, Culture, Sports, Science and Technology in Japan.

References

1. Paget SJ. On disease of the mammary areola preceding cancer of the mammary gland. St. Bartholomew’s Hosp Rep. 1874; 10:87–9.

2. Kanitakis J. Mammary and extramammary Paget's disease. J Eur Acad Dermatol Venereol. 2007; 21:581–90.

3. Herrel LA, Weiss AD, Goodman M, Johnson TV, Osunkoya AO, Delman KA, et al. Extramammary Paget's disease in males: survival outcomes in 495 patients. Ann Surg Oncol. 2015; 22:1625–30.

4. Karam A, Dorigo O. Treatment outcomes in a large cohort of patients with invasive Extramammary Paget's disease. Gynecol Oncol. 2012; 125:346–51.

5. Hatta N, Yamada M, Hirano T, Fujimoto A, Morita R. Extramammary Paget's disease: treatment, prognostic factors and outcome in 76 patients. Br J Dermatol. 2008; 158:313–8.

6. Hirakawa S, Detmar M, Kerjaschki D, Nagamatsu S, Matsuo K, Tanemura A, et al. Nodal lymphangiogenesis and metastasis: Role of tumor-induced lymphatic vessel activation in extramammary Paget's disease. Am J Pathol. 2009; 175:2235–48.

7. Ohara K, Fujisawa Y, Yoshino K, Kiyohara Y, Kadono T, Murata Y, et al. A proposal for a TNM staging system for extramammary Paget disease:

Retrospective analysis of 301 patients with invasive primary tumors. J Dermatol Sci. 2016 Sep;83(3):234–9.

8. Oashi K, Tsutsumida A, Namikawa K, Tanaka R, Omata W, Yamamoto Y, et al. Combination chemotherapy for metastatic extramammary Paget disease. Br J Dermatol. 2014; 170:1354–7.

9. Tokuda Y, Arakura F, Uhara H. Combination chemotherapy of low-dose 5-fluorouracil and cisplatin for advanced extramammary Paget's disease. Int J Clin Oncol. 2015; 20:194–7.

10. Yoshino K, Fujisawa Y, Kiyohara Y, Kadono T, Murata Y, Uhara H, et al. Usefulness of docetaxel as first-line chemotherapy for metastatic extramammary Paget's disease. J Dermatol. 2016; 43:633–7.

11. Kato M, Yoshino K, Maeda T, Nagai K, Oaku S, Hiura A, et al. Single-agent taxane is useful in palliative chemotherapy for advanced extramammary Paget’s disease; A Case Series. Br J Dermatol. 2019; 181:831–2.

12. Hirai I, Tanese K, Nakamura Y, Ishii M, Kawakami Y, Funakoshi T. Combination Cisplatin-Epirubicin-Paclitaxel Therapy for Metastatic Extramammary Paget's Disease. Oncologist. 2019; 24:e394–6.

13. Karam A, Berek JS, Stenson A, Rao J, Dorigo O. HER-2/neu targeting for recurrent vulvar Paget’s disease: a case report and literature review. Gynecol

Oncol. 2008; 111:568–71.

14. Takahagi S, Noda H, Kamegashira A, et al. Metastatic extramammary Paget's disease treated with paclitaxel and trastuzumab combination chemotherapy. J Dermatol. 2009 36:457–61.

15. Vornicova O, Hershkovitz D, Yablonski-Peretz T, Ben-Itzhak O, Keidar Z, Bar-Sela G. Treatment of metastatic extramammary Paget's disease associated with adnexal adenocarcinoma, with anti-HER2 drugs based on genomic alteration ERBB2 S310F. Oncologist. 2014; 19:1006–7.

16. Bertotti A, Migliardi G, Galimi F, Sassi F, Torti D, Isella C, et al. A molecularly annotated platform of patient-derived xenografts ("xenopatients") identifies HER2 as an effective therapeutic target in cetuximab-resistant colorectal cancer. Cancer Discov. 2011; 1:508–23.

17. Hidalgo M, Amant F, Biankin AV, Budinská E, Byrne AT, Caldas C, et al. Patient-derived xenograft models: an emerging platform for translational cancer research. Cancer Discov. 2014; 4:998–1013.

18. Koga Y, Ochiai A. Systematic Review of Patient-Derived Xenograft Models for Preclinical Studies of Anti-Cancer Drugs in Solid Tumors. Cells. 2019; 8:E418.

19. Nishi M, Tashiro M, Yoshida H. Stimulation of growth by both androgen and estrogen of the EMP-K1 transplantable tumor with androgen and estrogen

receptors from human extramammary Paget's disease in nude mice. J Natl Cancer Inst. 1992; 84:519–23.

20. Twelves C, Cortes J, Vahdat L, Olivo M, He Y, Kaufman PA, et al. Efficacy of eribulin in women with metastatic breast cancer: a pooled analysis of two phase 3 studies. Breast Cancer Res Treat. 2014; 148:553–61.

21. Richter CE, Hui P, Buza N, Silasi DA, Azodi M, Santin AD, et al. HER-2/NEU overexpression in vulvar Paget disease: the Yale experience. J Clin Pathol. 2010; 63:544–7.

22. Tanaka R, Sasajima Y, Tsuda H, Namikawa K, Tsutsumida A, Otsuka F, et al. Human epidermal growth factor receptor 2 protein overexpression and gene amplification in extramammary Paget disease. Br J Dermatol. 2013; 168:1259–66.

23. Tanaka R, Sasajima Y, Tsuda H, Namikawa K, Takahashi A, Tsutsumida A, et al. Concordance of the HER2 protein and gene status between primary and corresponding lymph node metastatic sites of extramammary Paget disease. Clin Exp Metastasis. 2016; 33:687–97.

24. Zhang G, Zhou S, Zhong W, Hong L, Wang Y, Lu S, et al. Whole-Exome Sequencing Reveals Frequent Mutations in Chromatin Remodeling Genes in Mammary and Extramammary Paget's Diseases. J Invest Dermatol. 2019;

139:789–795.

25. Kiniwa Y, Yasuda J, Saito S, Saito R, Motoike IN, Danjoh I, et al. Identification of genetic alterations in extramammary Paget disease using whole exome analysis. J Dermatol Sci. 2019; 94:229–235.

26. Tate JG, Bamford S, Jubb HC, Sondka Z, Beare DM, Bindal N, et al. COSMIC: the Catalogue Of Somatic Mutations In Cancer. Nucleic Acids Res. 2019; 47:D941–7.

27. Greulich H, Kaplan B, Mertins P, Chen TH, Tanaka KE, Yun SH, et al. Functional analysis of receptor tyrosine kinase mutations in lung cancer identifies oncogenic extracellular domain mutations of ERBB2. Proc Natl Acad Sci U S A. 2012; 109:14476–81.

28. Ma CX, Bose R, Gao F, Freedman RA, Telli ML, Kimmick G, et al. Neratinib Efficacy and Circulating Tumor DNA Detection of HER2 Mutations in HER2 Nonamplified Metastatic Breast Cancer. Clin Cancer Res. 2017; 23:5687–95.

29. Kavuri SM, Jain N, Galimi F, Cottino F, Leto SM, Migliardi G, et al. HER2 activating mutations are targets for colorectal cancer treatment. Cancer Discov. 2015; 5:832–41.

30. Hyman DM, Piha-Paul SA, Won H, Won H, Rodon J, Saura C, et al. HER kinase inhibition in patients with HER2- and HER3-mutant cancers. Nature.

2018; 554:189–194.

31. Towle MJ, Nomoto K, Asano M, Kishi Y, Yu MJ, Littlefield BA. Broad spectrum preclinical antitumor activity of eribulin (Halaven(R)): optimal effectiveness under intermittent dosing conditions. Anticancer Res. 2012; 32:1611–9.

32. Takeichi T, Okuno Y, Matsumoto T, Tsunoda N, Suzuki K, Tanahashi K, et al. Frequent FOXA1-Activating Mutations in Extramammary Paget's Disease. Cancers (Basel). 2020; 12(4).

33. Yanagi T, Krajewska M, Matsuzawa S, Reed JC. PCTAIRE1 phosphorylates p27 and regulates mitosis in cancer cells. Cancer Res 2014; 74:5795–807.

34. Ivanics T, Bergquist JR, Liu G, Kim MP, Kang Y, Katz MH, et al. Patient-derived xenograft cryopreservation and reanimation outcomes are dependent on cryoprotectant type. Lab Invest. 2018; 98:947–956.

35. Yanagi T, Watanabe M, Hata H, Kitamura S, Imafuku K, Yanagi H, et al. Loss of TRIM29 Alters Keratin Distribution to Promote Cell Invasion in Squamous Cell Carcinoma. Cancer Res. 2018; 78:6795-6806.

36. Wolff AC, Hammond MEH, Allison KH, Harvey BE, Mangu PB, Bartlett JMS, et al. Human Epidermal Growth Factor Receptor 2 Testing in Breast Cancer: American Society of Clinical Oncology/College of American Pathologists

Clinical Practice Guideline Focused Update. J Clin Oncol. 2018; 36: 2105–22.

37. Wainberg ZA, Anghel A, Desai AJ, Ayala R, Luo T, Safran B, et al. Lapatinib, a dual EGFR and HER2 kinase inhibitor, selectively inhibits HER2-amplified human gastric cancer cells and is synergistic with trastuzumab in vitro and in vivo. Clin Cancer Res. 2010; 16:1509–19.

38. Nonagase Y, Yonesaka K, Kawakami H, Watanabe S, Haratani K, Takahama T, et al. Heregulin-expressing HER2-positive breast and gastric cancer exhibited heterogeneous susceptibility to the anti-HER2 agents lapatinib, trastuzumab and T-DM1. Oncotarget. 2016; 7:84860–71.

39. Hendrikx JJ, Lagas JS, Song JY, Rosing H, Schellens JHM, Beijnen JH, et al. Ritonavir inhibits intratumoral docetaxel metabolism and enhances docetaxel antitumor activity in an immunocompetent mouse breast cancer model. Int J Cancer. 2016; 138:758–69.

Figure legends

Figure 1. Schematic of the study method

Tissue obtained from the EMPD patient is transplanted into NOD/Scid mice (generation 0: G0). The xenografted tumors are transplanted to further generations (G1-G4) and used for cell culture, histopathological analysis, genetic analysis, and treatment experiments.

Figure 2. The clinical manifestations and immunohistopathological findings for the primary site, the metastatic lymph node, and EMPD-PDX-H1

A, Clinical photo of the patient's primary tumor. B, Computed tomography image of the patient's lymph node metastasis (yellow arrow) and the clinical photo (inset). C, Appearance of the xenografted tumor on a NOD/Scid mouse (red arrowheads). D, Hematoxylin and eosin staining and immunohistochemistry of CK7 and HER2. The score for HER2 expression in invasive tumor cells was 1+, which is consistent with that in PDX tissue. Scale bar = 100 μm.

Figure 3. EMPD-PDX-H1 tumors harbor *ERBB2* gene mutations identical to those of the patient's primary and metastatic tumors.

A, Actionable genetic alterations in the patient's samples and EMPD-PDX-H1 tumors through deep sequencing using a comprehensive cancer panel. Identical gene alterations

(*ERBB2* p.S310F) are detected in original patient's tumor samples (lymph node metastasis: LN), PDX (G1), and PDX (G2). B, Sanger sequencing results. An identical *ERBB2* mutation is detected in the patient's primary tumor.

Figure 4. HER2-targeted therapies suppress the tumor growth of EMPD-PDX-H1 harboring the *ERBB2* S310F mutation.

Tumor-bearing NOD/Scid mice were randomized into no therapy, lapatinib 100 mg/kg/day orally (A, B), trastuzumab 10 mg/kg intraperitoneally twice a week (C, D), or a combination of these two agents (E, F). Green arrowheads indicate the injection of trastuzumab. Tumor volumes and weights were calculated and analyzed as indicated in Materials and Method. The results are presented as means, with the error bars representing the SD from the mean. All comparisons were statistically significant between the following groups: combo, trastuzumab or lapatinib versus no therapy.

Figure 5. EMPD-PDX-H1 are sensitive to cytotoxic agents, including eribulin and docetaxel.

Treatment experiments of cytotoxic agents using EMPD-PDX-H1. Tumor-bearing NOD/Scid mice were randomly treated with one of following injections: docetaxel at 20 mg/kg once a week (A, B), eribulin at 1.5 mg/kg once a week (C, D), eribulin at 0.45

503 mg/kg (E, F) or sterile PBS once a week (control). The results are presented as means,
504 with the error bars representing the SD from the mean. All comparisons are statistically
505 significant between the following groups: the docetaxel group or the eribulin groups
506 versus the control, $P < 0.001$. Blue, green, and red arrowheads indicate the injection of
507 docetaxel, eribulin 1.5 mg/kg or eribulin at 0.45 mg/kg, respectively.

Maeda et al.
Figure 1

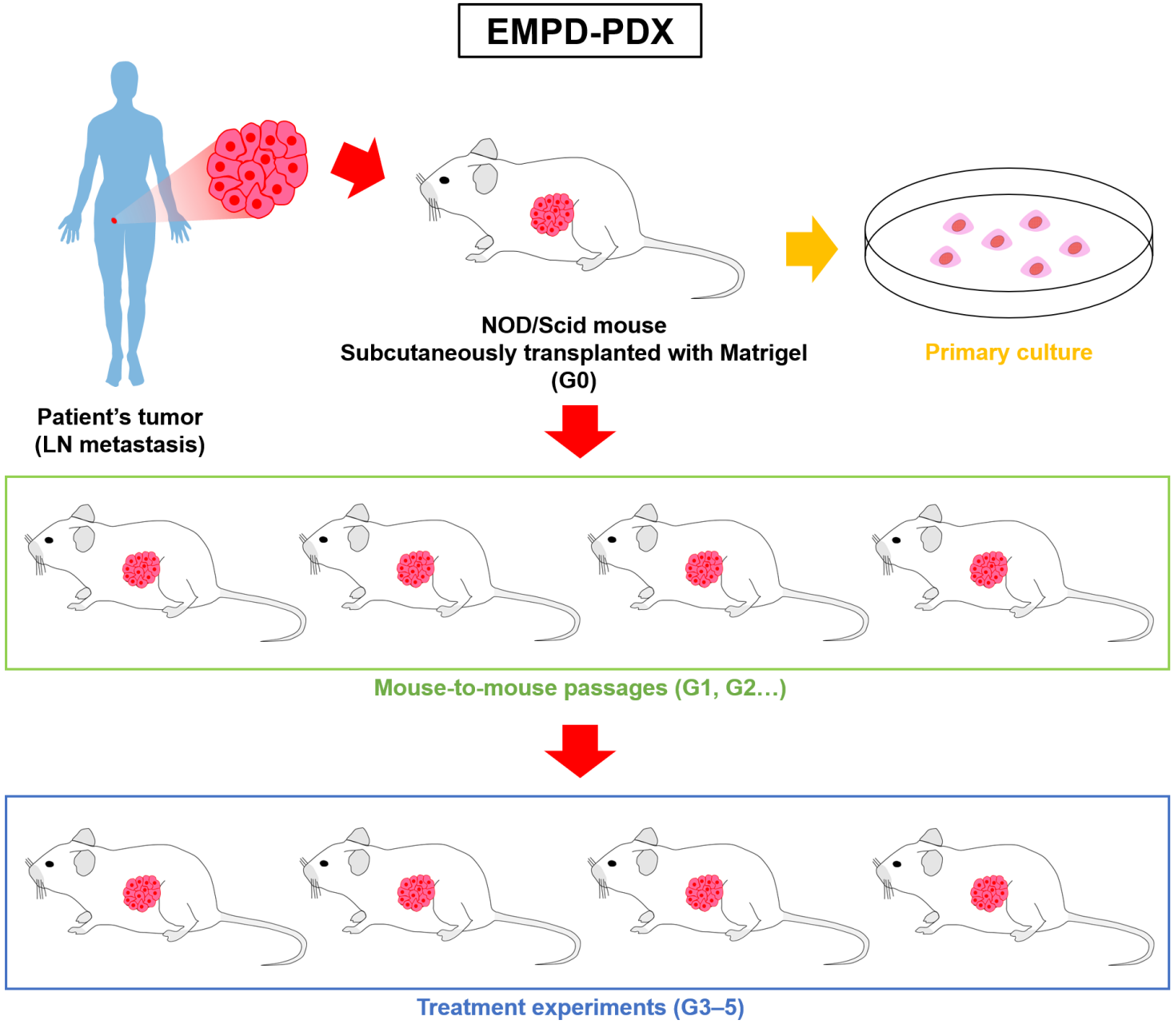

Maeda et al.
Figure 2

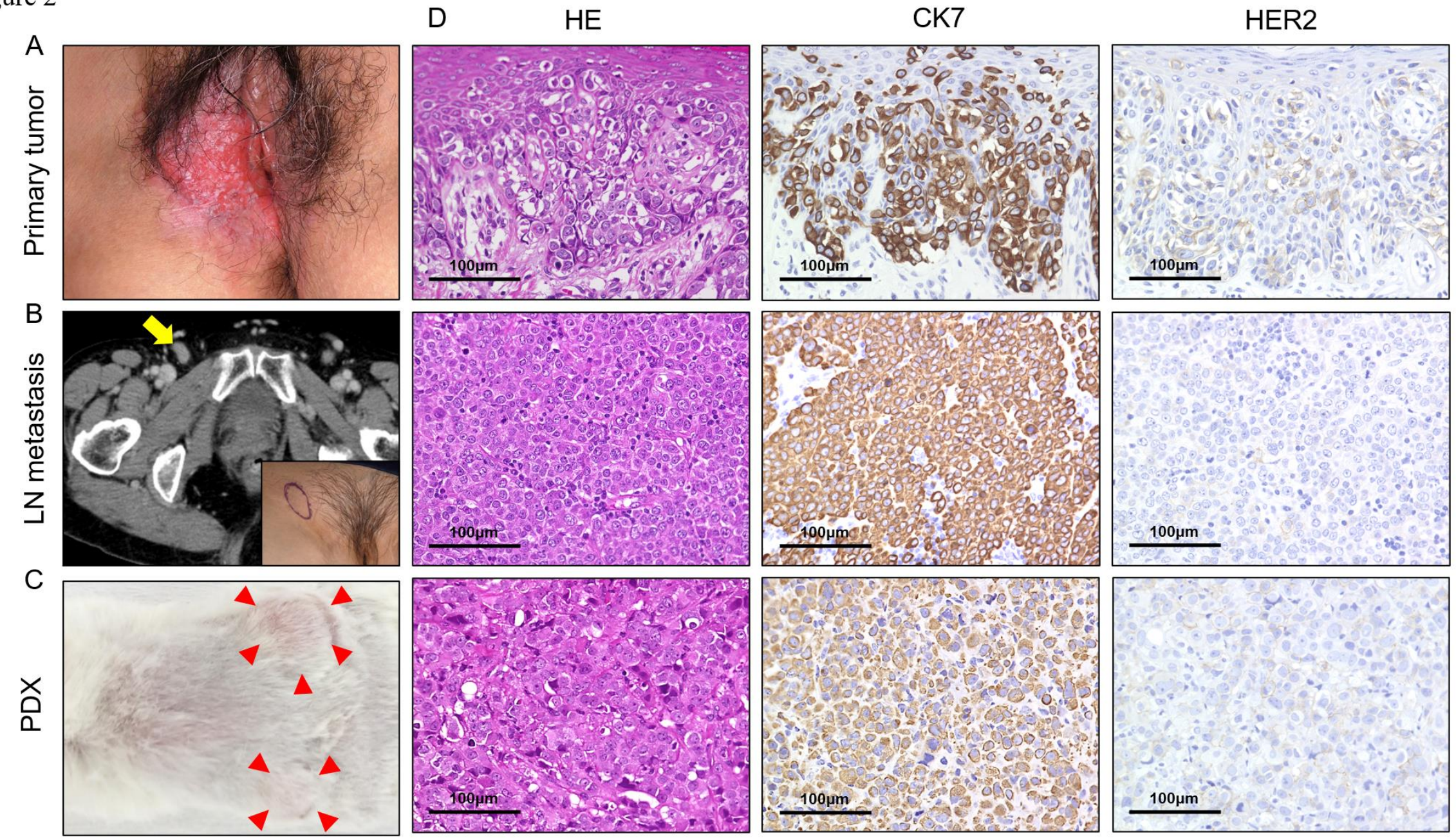

Maeda et al.
Figure 3

A

Sample characteristics	Major gene alterations (VAF, %)
Patient's blood	None
Patient's LN	*ERBB2* S310F (51.6%)
PDX (G1)	*ERBB2* S310F (70.7%)
PDX (G2)	*ERBB2* S310F (68.5%)

VAF: variant allele frequency

B **_ERBB2_ S310F (c.929C>T)**

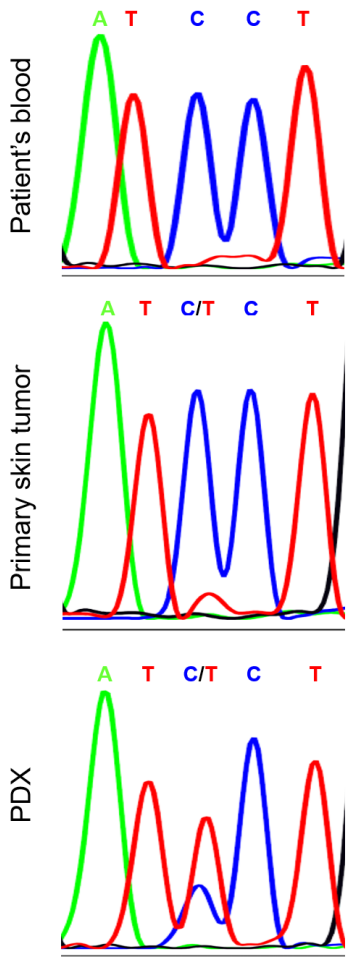

Maeda et al.
Figure 4

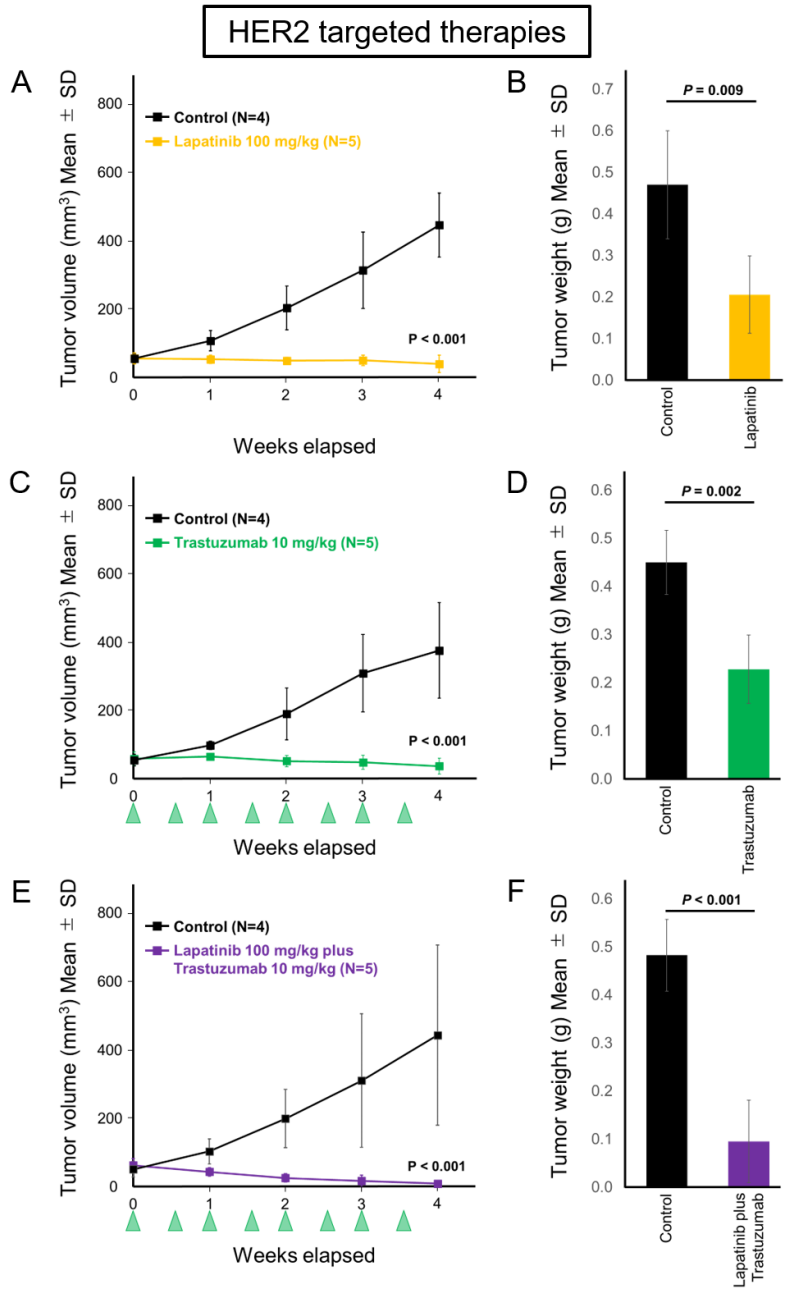

Maeda et al.
Figure 5